Available online at www.sciencedirect.com
ScienceDirect
Polymer 49 (2008) 703–714
polymer
www.elsevier.com/locate/polymer

Synthesis and characterization of novel polyazomethines containing perylene units

İsmet Kaya*, Sermet Koyuncu, Süleyman Çulhaoğlu

Department of Chemistry, Faculty of Sciences and Arts, Çanakkale Onsekiz Mart University, TR-17020 Çanakkale, Turkey

Received 10 August 2007; received in revised form 27 November 2007; accepted 8 December 2007
Available online 7 January 2008

Abstract

Polyazomethines including perylene units in the main chain were synthesized via polycondensation of diaminoperylene with aromatic dialdehydes. UV/vis, FT-IR, ^{1}H NMR, ^{13}C NMR and elemental analysis techniques were carried out for the characterization of the synthesized diaminoperylene, dialdehydes and polyazomethines including perylene units (PAM-PERs). The number-average molecular weight (M_n), weight-average molecular weight (M_w) and polydispersity index (PDI) values of PAM-PERs were determined by size exclusion chromatography (SEC). Thermal properties of PAM-PERs was determined by using TGA/DTA and DSC systems. The highest occupied molecular orbital (HOMO) and the lowest unoccupied molecular orbital (LUMO) energy levels, and electrochemical (E'_g) and optical (E_g) band gap values were calculated by using the results of cyclic voltammetry and UV/vis, respectively. Conductivity measurements of PAM-PERs were carried out with electrometer by using four-point probe technique. The conductivity was observed to be increased by doping agent iodine.

Keywords: Polyazomethines; Perylene; Conducting polymer

1. Introduction

Polyazomethines (PAMs), known as polyimines or Schiff bases, were prepared for the first time by Adams and co-workers from terephthalaldehyde, benzidine and dianisidine in 1923 [1]. Polyazomethines, which contain −HC═N bonds in their structure, may exhibit attractive physical properties such as electronic, optoelectronic, nonlinear optical or liquid crystalline that make this kind of polymers interesting particularly in materials science [2–6]. Polyazomethines have also high thermal stability [7], high mechanical strength [8,9] and ability to form metal chelates [10–12]. Many of these polymers form mesophases on heating [13]. This type of material has drawbacks such as low solubility in common organic solvents and high melting temperature, which make its processing difficult. However, several approaches have been undertaken to improve the processability of conjugated polyazomethines by introducing various substituted benzene rings in the main chain [14,15], by using monomers containing certain heterocyclic units such as thiophene [16], oxadiazole, thiadiazole [17–19], pyridine [20], diphenylfluorene [21] and others. Copolymers with phenyl-substituted quinoxaline rings proved to be very beneficial [22,23]. Dendritic phenyl-azomethines supply a good solution, because of their frameworks around various functional cores [24,25].

Perylene bisimides are important representative class of n-type semiconductors that form some of the most environmentally and thermally stable materials that can be used as nonlinear optical devices, electrochromic or smart windows, photo-resists, optical modulators and valves, imaging materials, nanoelectronic and optical devices, and transistors [26–31]. Furthermore, perylene bisimides have been used as electron acceptors in many fundamental studies of photo-induced electron-transfer including models for photosynthesis, solar energy conversion, molecular electronics, electrochromic devices, and photorefractive materials because of high electron affinity and excellent transport properties [32–35]. These molecules have been widely used in

* Corresponding author. Tel.: +90 286 2180018/1858; fax: +90 286 2180533.
E-mail address: kayaismet@hotmail.com (İ. Kaya).

0032-3861/$ - see front matter © 2007 Elsevier Ltd. All rights reserved.
doi:10.1016/j.polymer.2007.12.010

electron-transfer studies because they undergo reversible one-electron reduction at modest potentials to form stable radical anions [36].

Synthesis of soluble and thermally stable azomethine polymers is very important. Despite the fact soluble polyimides [37,38], polyesters [39] and polyurethanes [40] containing perylene units were synthesized previously. This report highlights only the first synthesis of polyazomethines containing perylene units in the literature. Due to selected dialdehydes, synthesized azomethine polymers are highly soluble in polar protic solvents and thermally stable.

We now report on the synthesis of some aliphatic/aromatic poly(Schiff base)s obtained from the polycondensation reaction of diaminoperylene with some different aromatic dialdehydes and reveal the group effects of the *ortho*- and *para*-phenyl ring position in the middle of DAs and the existence of methoxy groups in the main chain. The characterizations of all compounds were made by UV/vis, FT-IR, ^{1}H NMR, ^{13}C NMR, SEC, TGA/DTA and elemental analysis techniques. Electrochemical and optical band gaps of PAM-PERs were calculated from the results of cyclic voltammetry and UV/vis measurements. Conductivity measurements were carried out by four-point probe technique.

2. Experimental

2.1. Materials

3,4:9,10-Perylenetetracarboxylicdianhydride (PDA), 2,5-dimethyl-*p*-phenylenediamine, *p*-hydroxy benzaldehyde, vanillin, *o*-xylenedibromide, *p*-xylenedibromide, tetrabutylammonium-hexafluorophosphate ($TBAPF_6$) and imidazole were obtained from Fluka. Dimethylformamide (DMF), dimethylsulfoxide (DMSO), *N*-methylpyrolidonone (NMP), methanol (MeOH), chloroform ($CHCl_3$), acetonitrile (CH_3CN), pyridine, sulfuric acid (H_2SO_4), hydrochloric acid (HCl), potassium hydroxide (KOH) and anhydrous potassium carbonate (K_2CO_3) were supplied from Merck chemical Co. (Germany).

2.2. Syntheses of dialdehyde molecules (DA-1–DA-4)

Dialdehyde molecules is synthesized according to the literature data [41]. Hydroxy benzaldehydes (6 mmol) dissolved in 30 ml of DMF were added into 250 ml three-necked flask equipped with a condenser and magnetic stir bar. Anhydrous sodium carbonate (7.5 mmol) was added to flask. *o*-Xylenedibromide or *p*-xylenedibromide (3 mmol) was dissolved in 30 ml DMF and added into the reaction mixture under argon atmosphere. The mixture was heated for 4 h at 150 °C with continuous stirring. After cooling, the product was poured into 250 ml cold water (approximately 5–10 °C). The precipitate was washed in 250 ml of hot water for three times for separating from mineral salts. Dialdehyde molecules were filtered, dried and finally, recrystallized from methanol and dried in vacuum desiccator for 24 h at 60 °C. Dialdehyde molecules were obtained according to the reactions presented in Scheme 1 (DA-1: 62.66%, 155–156 °C; DA-2: 56.78%, 161–163 °C; DA-3: 59.37%, 166–167 °C; DA-4: 48.63%, 142–143 °C).

2.2.1. DA-1

UV/vis (λ_{max}) (MeOH): 206, 232, 273 and 307 nm. FT-IR (cm^{-1}): 3067 (C–H aromatic) 2937 (C–H aliphatic), 2854, 1681 (C=O aldehyde), 1583, 1506, 1464 (C=C phenyl), 1267 (CH_2–O ether). ^{1}H NMR (DMSO-d_6): δ ppm, 9.85 (s, 2H, –CHO), 7.42 (s, 2H, Ar–$H_{aa'}$), 7.55 (d, 2H, Ar–$H_{bb'}$), 7.28 (d, 2H, Ar–$H_{cc'}$), 7.51 (s, 4H, H_d), 5.24 (s, 4H, –OCH_2–), 3.84 (s, 6H, –OCH_3). ^{13}C NMR (DMSO-d_6): δ ppm, 191.86 (C1), 130.29 (C2), 126.38 (C3), 113.07 (C4), 153.57 (C5), 149.86 (C6), 110.15 (C7), 56.02 (C8), 70.19 (C9), 136.69 (C10), 128.61 (C11). Calcd. for $C_{24}H_{22}O_6$: C, 70.92; H, 5.46; O, 23.62. Found: C, 70.42; H, 5.17; O, 24.11.

2.2.2. DA-2

UV/vis (λ_{max}) (MeOH): 205, 229, 274 and 308 nm. FT-IR (cm^{-1}): 3074 (C–H aromatic), 2919, 2811 (C–H aliphatic), 1675 (C=O aldehyde), 1582, 1512, 1466 (C=C phenyl), 1265 (CH_2–O ether). ^{1}H NMR (DMSO-d_6): δ ppm, 9.83 (s, 2H, -CHO), 7.55 (s, 2H, Ar–$H_{aa'}$), 7.52 (d, 2H, Ar–$H_{bb'}$), 7.38 (d, 2H, Ar–$H_{cc'}$), 7.42 (d, 2H, $H_{dd'}$), 7.38 (d, 2H, $H_{ee'}$), 5.40 (s, 4H, –OCH_2), 3.82 (s, 6H, –OCH_3). ^{13}C NMR (DMSO-d_6): δ ppm, 191.82 (C1), 129.09 (C2), 126.24 (C3), 110.07 (C4), 153.38 (C5), 149.91 (C6), 113.16 (C7), 56.02 (C8), 68.53 (C9), 135.12 (C10), 130.39 (C11), 128.81 (C12). Calcd. for $C_{24}H_{22}O_6$: C, 70.92; H, 5.46; O, 23.62. Found: C, 70.33; H, 5.08; O, 24.24.

2.2.3. DA-3

UV/vis (λ_{max}) (MeOH): 204, 219 and 282 nm. FT-IR (cm^{-1}): 3077 (C–H aromatic), 2955, 2883 (C–H aliphatic), 1674 (C=O aldehyde), 1600, 1573, 1525 (C=C phenyl), 1241 (CH_2–O ether). ^{1}H NMR (DMSO-d_6): δ ppm, 9.88 (s, 2H, –CHO), 7.87 (d, 4H, Ar–$H_{aa'}$), 7.10 (d, 4H, Ar–$H_{bb'}$), 7.49 (s, 4H, Ar–H_c), 5.18 (s, 4H, –OCH_2). ^{13}C NMR (DMSO-d_6): δ ppm, 190.69 (C1), 129.86 (C2), 131.86 (C3), 115.29 (C4), 163.47 (C5), 70.70 (C6), 135.83 (C7), 127.70 (C8). Calcd. for $C_{22}H_{18}O_4$: C, 76.29; H, 5.24; O, 18.48. Found: C, 76.03; H, 5.21; O, 17.99.

2.2.4. DA-4

UV/vis (λ_{max}) (MeOH): 206, 217 and 282 nm. FT-IR (cm^{-1}): 3074 (C–H aromatic), 2915, 2828 (C–H aliphatic), 1678 (C=O aldehyde), 1597, 1578, 1511 (C=C phenyl), 1266 (CH_2–O ether). ^{1}H NMR (DMSO-d_6): δ ppm, 9.89 (s, 2H, -CHO), 7.84 (d, 4H, Ar–$H_{aa'}$), 7.09 (d, 4H, Ar–$H_{bb'}$), 7.54 (d, 2H, Ar–$H_{cc'}$), 7.44 (t, 2H, Ar–$H_{dd'}$), 5.28 (s, 4H, –OCH_2). ^{13}C NMR (DMSO-d_6): δ ppm, 190.71 (C1), 129.00 (C2), 133.14 (C3), 115.00 (C4), 163.57 (C5), 68.43 (C6), 134.29 (C7), 130.43 (C8), 129.43 (C9). Calcd. for $C_{22}H_{18}O_4$: C, 76.29; H, 5.24; O, 18.48. Found; C, 76.21; H, 5.18; O, 18.32.

2.3. Synthesis of N,N-(2,5-dimethyl-4-aminophenyl)-perylene-3,4:9,10-dicarboximide (DAPDI)

PDA (3.93 g, 10 mmol), 2,5-dimethyl-*p*-phenylenediamine (6.8 g, 50 mmol) and imidazole (5 g, 77.5 mmol) were added

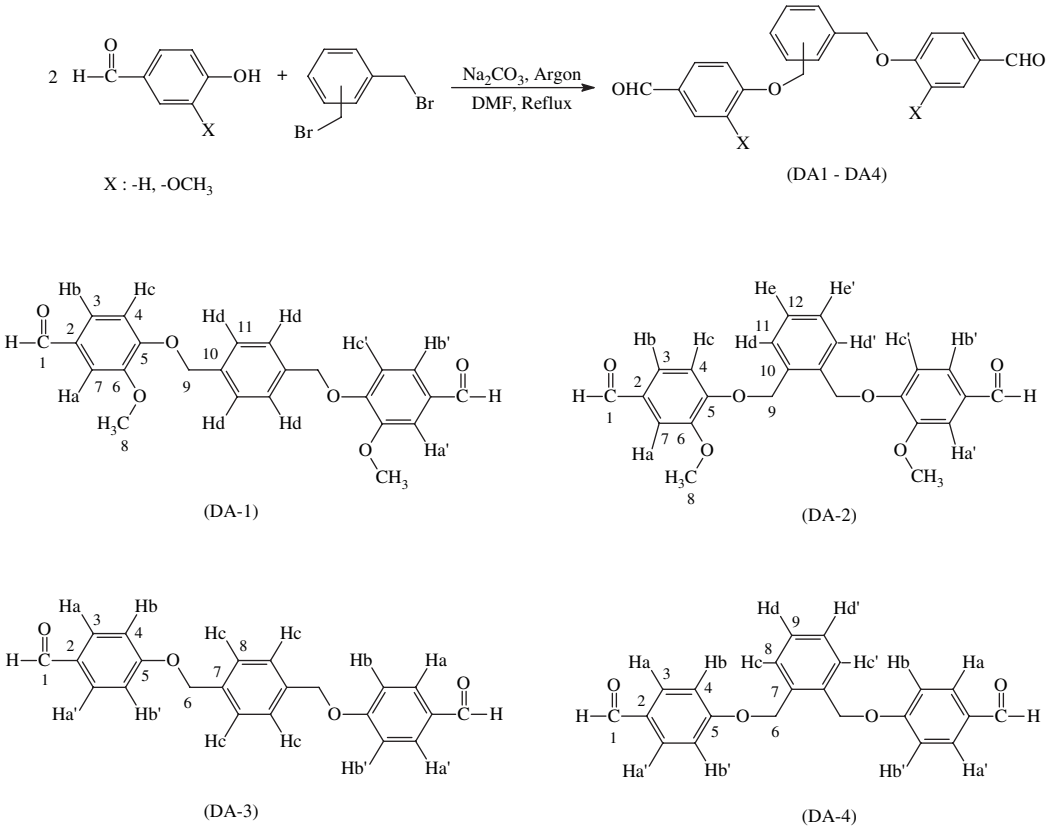

Scheme 1.

to 100 ml dry pyridine and refluxed under argon atmosphere. After 6 h, this mixture was cooled to room temperature and poured into the mixture of 25 ml water, 30 ml $CHCl_3$ and 10 drops of HCl. The aqueous fraction was separated and then re-extracted three times with $CHCl_3$. Organic fractions were combined and washed with dilute $NaHCO_3$. The solvent is stripped of by a rotary evaporator and the residue separated by chromatography on silica gel (DAPDI: v/v, 1/10 MeOH/$CHCl_3$ as eluent, 0.98 g, yield 62%).

UV/vis (λ_{max}) ($CHCl_3$): 233, 260, 459, 490 and 527 nm; FT-IR (cm^{-1}): 3437, 3366 (−NH_2 amine), 3088 (C−H phenyl), 2965, 2921 (C−H aliphatic), 1698, 1656 (C═O imide), 1591, 1575, 1514 (C═C phenyl). ^{1}H NMR ($CHCl_3$-*d*): δ ppm, 8.68 (d, 4H, Ar−$H_{aa'}$, $H_{bb'}$), 8.61 (d, 4H, Ar−$H_{cc'}$, $H_{dd'}$), 7.19 (s, 2H, Ar−$H_{ee'}$), 6.92 (s, 2H, Ar−$H_{ff'}$), 3.99 (4H, −NH_2), 2.81 (s, 6H, C−H aliphatic), 2.52 (s, 6H, C−H aliphatic). Calcd. for $C_{40}H_{28}N_4O_4$: C, 76.42; H, 4.49; N, 8.91; O, 10.18. Found: C, 76.30; H, 4.38; N, 8.88; O, 10.03.

2.4. Syntheses of polyazomethines containing perylene units

Into a 250 ml three-necked round bottom-flask equipped with a reflux condenser, a gas inlet−outlet, a Dean−Stark trap and a magnetic stirrer is added DAPDI (0.628 g, 1 mmol) and 20 ml dry DMF under argon atmosphere and heated to 100 °C. After 10 min, dialdehyde molecules (DA-1: 0.346 g, 1 mmol; DA-2: 0.346 g, 1 mmol; DA-3: 0.406 g, 1 mmol; or DA-4: 0.406 g, 1 mmol) in 10 ml dry DMF was added drop wise. The solution was refluxed for 10 h and then cooled to room temperature. After cooling to room temperature the polymer was precipitated into 150 ml methanol/water (v/v, 1:1) mixture, washed with methanol and dried at 60 °C for 10 h in a vacuum oven. Yields of compounds: PAM-PER-1: 0.632 g, 64.6%; PAM-PER-2: 0.686 g, 70.1%; PAM-PER-3: 0.702 g, 67.8%; PAM-PER-4: 0.612 g, 59.1%.

2.4.1. PAM-PER-1

UV/vis (λ_{max}) ($CHCl_3$): 261, 276, 310, 459, 490 and 527 nm. FT-IR (cm^{-1}): 3080, 3063 (C−H aromatic), 2921, 2860, 2845 (C−H aliphatic), 1701, 1658 (C═O imide), 1630 (C═N imine), 1594, 1575, 1463 (C═C phenyl), 1245 (CH_2−O ether). ^{1}H NMR ($CHCl_3$-*d*): δ ppm, 9.77 (s, 1H, −CHO; end group), 8.41 (s, 2H, CH═N), 8.67−8.59 (m, 8H, Ar−H; perylene), 7.39−6.62 (m, 14H, Ar−H; phenyl), 5.16 (s, 4H, O−CH_2), 3.87 (s, 6H, O−CH_3), 3.72 (s, 2H, −NH_2; end group), 2.01 (s, 3H, Ar−CH_3), 1.18 (s, 3H, Ar−CH_3). ^{13}C NMR ($CHCl_3$-*d*): δ ppm, 190.82, 163.55, 153.51, 150.16, 136.14, 131.78, 130.46, 129.95, 127.73, 127.62, 126.45, 123.26, 123.87, 117.07, 112.48, 109.54, 70.58, 56.07, 17.32. Calcd. for $(C_{64}H_{46}N_5O_8)_n$: C, 75.87; H, 4.57; N, 6.91; O, 12.63. Found: C, 75.16; H, 4.57; N, 6.91; O, 12.63.

2.4.2. PAM-PER-2

UV/vis (λ_{max}) ($CHCl_3$): 260, 275, 309, 459, 490 and 527 nm. FT-IR (cm^{-1}): 3078, 3054 (C−H phenyl), 2936, 2874, 2845

(C–H aliphatic), 1701, 1658 (C=O imide), 1634 (C=N imine), 1598, 1575, 1463 (C=C phenyl), 1267 (CH_2–O ether). ^{1}H NMR ($CHCl_3$-*d*): δ ppm, 9.84 (s, 1H, –CHO; end group), 8.56 (s, 2H, CH=N), 8.67–8.59 (m, 8H, Ar–H; perylene), 7.62–6.73 (m, 14H, Ar–H; phenyl), 5.34 (s, 4H, O–CH_2), 3.91 (s, 6H, O–CH_3), 3.72 (s, 2H, –NH_2; end group), 2.08 (s, 3H, Ar–CH_3), 1.24 (s, 3H, Ar–CH_3). ^{13}C NMR ($CHCl_3$-*d*): δ ppm, 190.74, 163.50, 153.33, 150.12, 134.24, 131.86, 131.22, 130.52, 128.89, 128.72, 126.33, 123.67, 123.25, 121.06, 117.07, 112.45, 109.41, 69.31, 55.93, 17.01. Calcd. for $(C_{64}H_{46}N_5O_8)_n$: C, 75.87; H, 4.57; N, 6.91; O, 12.63. Found: C, 75.33; H, 4.44; N, 6.82; O, 12.47.

2.4.3. PAM-PER-3

UV/vis (λ_{max}) ($CHCl_3$): 240, 277, 466, 490 and 526 nm. FT-IR (cm^{-1}): 3067, 3044 (C–H phenyl), 2921, 2855 (C–H aliphatic), 1701, 1658 C=O imide), 1621 (C=N imine), 1594, 1571, 1463 (C=C phenyl), 1244 (CH_2–O ether). ^{1}H NMR ($CHCl_3$-*d*): δ ppm, 9.77 (s, 1H, –CHO; end group), 8.45 (s, 2H, CH=N), 8.67–8.59 (m, 8H, Ar–H; perylene), 7.82–6.64 (m, 16H, Ar–H; phenyl), 5.08 (s, 4H, O–CH_2), 3.64 (s, 2H, –NH_2; end group), 2.14 (s, 3H, Ar–CH_3), 1.19 (s, 3H, Ar–CH_3). ^{13}C NMR ($CHCl_3$-*d*): δ ppm, 190.65, 164.23, 145.56, 139.24, 134.17, 133.52, 132.64, 128.94, 126.27, 122.81, 121.82, 119.21, 118.09, 115.72, 70.39, 17.77. Calcd. for $(C_{62}H_{42}N_5O_8)_n$: C, 75.60; H, 4.29; N, 7.11; O, 12.98. Found: C, 75.33; H, 4.44; N, 7.01; O, 12.67.

2.4.4. PAM-PER-4

UV/vis (λ_{max}) ($CHCl_3$): 240, 274, 461, 489 and 526 nm. FT-IR (cm^{-1}): 3068, 3034 (C–H aromatic), 2921, 2860, 2845 (C–H aliphatic), 1701, 1658 (C=O imide), 1630 (C=N imine), 1594, 1575, 1463 (C=C phenyl), 1245 (CH_2–O ether). ^{1}H NMR ($CHCl_3$-*d*): δ ppm, 9.77 (s, 1H, –CHO; end group), 8.41 (s, 2H, CH=N), 8.67–8.59 (m, 8H, Ar–H; perylene), 7.99–6.43 (m, 16H, Ar–H; phenyl), 5.24 (s, 4H, O–CH_2), 3.72 (s, 2H, –NH_2; end group), 1.99 (s, 3H, Ar–CH_3), 1.04 (s, 3H, Ar–CH_3). ^{13}C NMR ($CHCl_3$-*d*): δ ppm, 190.52, 163.78, 144.89, 139.16, 133.97, 133.26, 131.93, 128.83, 128.69, 126.18, 122.74, 121.59, 119.17, 117.88, 115.66, 70.28, 17.53. Calcd. for $(C_{62}H_{42}N_5O_8)_n$: C, 75.60; H, 4.29; N, 7.11; O, 12.98. Found: C, 75.40; H, 4.39; N, 6.97; O, 12.55.

2.5. Electrochemical properties

Electrochemical properties of the initial compounds and polyazomethines were determined by CH Instruments 660C cyclic voltammeter. The electrochemical cell consist of an Ag wire pseudo-reference electrode (RE), Pt wire as counter electrode (CE) and glassy carbon working electrode (WE) immersed in 0.1 M $TBAPF_6$ as supporting electrolyte. The experiments were carried under argon atmosphere. The potentials were calibrated to the ferrocene redox couple $E^{\circ}(Fc/Fc^{+}) = +0.41$ V vs. Ag/Ag^{+}. All reported potentials were given vs. Ag/Ag^{+} [35]. The HOMO and LUMO energy levels and electrochemical band gaps (E'_g) of synthesized compounds were calculated from their oxidation and reduction onset values.

2.6. Electrical properties

Conductivity was measured on a Keithley 2400 Electrometer. The pellets were pressed on hydraulic press developing up to 1687.2 kg/cm^2. Iodine doping was carried out by exposure of the pellets to iodine vapor at atmospheric pressure and room temperature in a desiccator [42].

2.7. Optical properties

UV/vis spectra of the compounds were measured by using Perkin–Elmer Lambda 25 spectrophotometer. The absorption spectra of the initial compounds and PAM-PERs were recorded in methanol and chloroform, respectively. The optical band gaps (E_g) of DAs, DAPDI and PAM-PERs were calculated from their absorption edges [35].

2.8. Solubility and measurements

Solubility test results of synthesized compounds are shown in Table 1. The infrared spectra were measured by Perkin–Elmer Spectrum One FT-IR system. The FT-IR spectra were recorded using universal ATR attachment sampling (powder form directly usable) accessory within the wavelengths of 4000–650 cm^{-1}. Synthesized compounds were characterized by elemental analysis (LECO-CHNS-932) and ^{1}H NMR (Bruker Avance DPX-400) recorded at 25 °C by using $CHCl_3$-*d* as solvent and TMS as internal standard. Thermal

Table 1
Solubility of synthesized compounds (0.05 g in 10 ml)

Compounds	NMP	DMSO	DMF	Ethyl Acetate	$CHCl_3$	Acetone	CH_3OH	CH_3CN	Toluene	Hexane
DA-1	+/+	+/+	+/+	+/+	+/+	+/+	+/+	+/+	–/+	–/–
DA-2	+/+	+/+	+/+	+/+	+/+	+/+	+/+	+/+	–/+	–/–
DA-3	+/+	+/+	+/+	+/+	–/+	–/+	–/+	+/+	–/–	–/–
DA-4	+/+	+/+	+/+	+/+	–/+	–/+	–/+	+/+	–/–	–/–
DAPDI	+/+	+/+	+/+	+/+	+/+	–/+	–/+	+/+	–/–	–/–
PAM-PER-1	+/+	+/+	+/+	+/+	+/+	+/+	–/+	+/+	–/–	–/–
PAM-PER-2	+/+	+/+	+/+	+/+	+/+	+/+	–/+	+/+	–/–	–/–
PAM-PER-3	+/+	+/+	+/+	+/+	+/+	–/+	–/+	+/+	–/–	–/–
PAM-PER-4	+/+	+/+	+/+	+/+	+/+	–/+	–/+	+/+	–/–	–/–

+/+: soluble at room temperature; –/+: soluble at heating; –/–: insoluble.

data were obtained by using Perkin–Elmer Diamond Thermal Analysis instrument. The DTA–TGA measurements were performed between 20 and 1000 °C (in N_2, rate 10 °C/min). The glass transition temperatures (T_g) of polymers were obtained by using Perkin–Elmer Sapphire DSC instrument. The DSC measurements were performed between 20 and 250 °C (in N_2, rate 20 °C/min). The number-average molecular weight (M_n), weight-average molecular weight (M_w) and polydispersity index (PDI) values of polymer were determined by size exclusion chromatography, SEC (Shimadzu Co., Japan). For SEC investigations a SGX 3.3 mm inside diameter × 300 mm columns were used with DMF (0.4 ml/min) as the eluent applied at polystyrene standards. A refractive index detector was used to analyze the product at 25 °C.

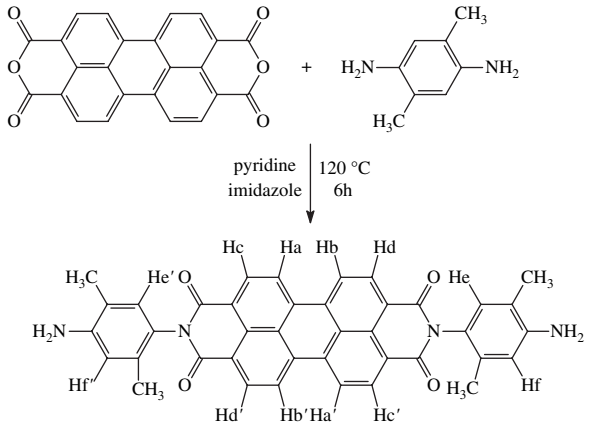

Scheme 2.

3. Results and discussion

3.1. Synthesis and characterization

Dialdehyde molecules (DAs) is synthesized according to the previously published procedure [37] from hydroxybenzaldehyde derivatives and xylenedibromide compounds as shown in Scheme 1. All of the DAs are white color as expected. The solubility of DA-1 and DA-2 is higher than the other DAs because of the $-OCH_3$ groups. While DA-1 and DA-2 compounds are soluble in common organic solvents such as methanol, ethanol, chloroform, ethyl acetate, acetone, DMF, DMSO and NMP, the others (DA-3 and DA-4) are partly soluble in ethanol, chloroform and acetone and in polar protic solvents such as ethyl acetate, DMF, DMSO and NMP. However, all of DAs are not soluble in apolar solvents, such as toluene, hexane, and heptane. Diaminoperylene compound (DAPDI) was prepared from the condensation reaction of excess amount of 2,5-dimethyl *p*-phenylenediamine with 3,4:9,10-perylenetetracarboxylicdianhydride (PDA). Excess of 2,5-dimethyl-*p*-phenylenediamine and formed polyimide at the end of this reaction were removed by column chromatography and the yield was found to be 62%. While PDA is not soluble in common organic solvents at the room temperature, synthesized DAPDI is soluble in chloroform, ethyl acetate, DMF, NMP and DMSO but partly soluble in methanol, ethanol and acetone. Dimethyl groups on phenyl rings and occurred imide bonds increase the solubility. PAM-PERs were synthesized from the polycondensation reaction of DAs with DAPDI. Also Dean–Stark trap is used to remove the water during the reaction. DAPDI could easily oxidize because of the diamine groups. To protect the polymerization of DAPDI on itself, all reactions were carried out in dry DMF under argon atmosphere. The products (PAM-PERs) are washed with methanol/water (v/v, 1:1) to remove the initial compounds and the yields of DA-1, DA-2, DA-3 and DA-4 were found to be 64.6, 70.1, 67.8, 59.1%, respectively. While these polymers (PAM-PERs) were taken place, the light red solution became dark red. All these reactions and solubility of corresponding products are shown in Schemes 1–3 and Table 1, respectively.

After completion of the synthetic works, all compounds were characterized by FT-IR, ^{1}H NMR and elemental analysis techniques. There are significant changes in the spectral properties of the initial compounds and the products. While some of the signals were disappeared, some new ones were appeared. In FT-IR spectrum of DAs, aliphatic C–H vibration exerted by $-OCH_2$ and $-OCH_3$ groups were observed in 2955–2811 cm^{-1}. Furthermore, characteristic aldehyde –C=O vibration for a carbonyl group were observed between 1681 and 1674 cm^{-1}. In the FT-IR spectra of the diaminoperylene compound (DAPDI) its characteristic imide –C=O vibrations were observed at 1698 and 1656 cm^{-1}. Also characteristic $-NH_2$ vibrations were clearly observed at 3437 and 3366 cm^{-1} in this spectrum. Finally, the FT-IR spectra of PAM-PERs, synthesized from the condensation reaction of DAPDI with DAs, showed the imine bond (–CH=N–) vibrations between 1634 and 1621 cm^{-1}.

Molecular structures of DAs, DAPDI and PAM-PERs were identified from their ^{1}H NMR spectra recorded in deuterated organic solvents such as DMSO-d_6 and $CHCl_3$-d. ^{1}H NMR spectra of PAM-PER-1, DA-1 and DAPDI were shown in Figs. 1–3, respectively, and these results indicate that all reactions were completed successfully.

SEC analyses of PAM-PERs were performed at 30 °C using DMF/MeOH (v/v, 4/1) as eluent at a flow rate of 0.4 ml/min. The M_n, M_w and PDI values of compounds were calculated according to a polystyrene standard calibration curve and are summarized in Table 2. According to the SEC analysis results, while PAM-PER-2 shows two fraction peaks, the others show three fraction peaks in their chromatograms. These polymers showed narrow molecular weight and distribution. Thus, PDI values of PAM-PERs were found to be 1.235, 1.375, 1.241 and 1.154, respectively.

3.2. Optical and electrochemical properties

The UV/vis spectra were recorded in $CHCl_3$ and methanol. The condensation of DAPDI with DAs did not change the perylene carbonyl specific absorption bands at 459, 490, 527 nm [36]. Thus optical band gap values of the PAM-PERs and DAPDI are found to be the same. PAM-PERs have shown

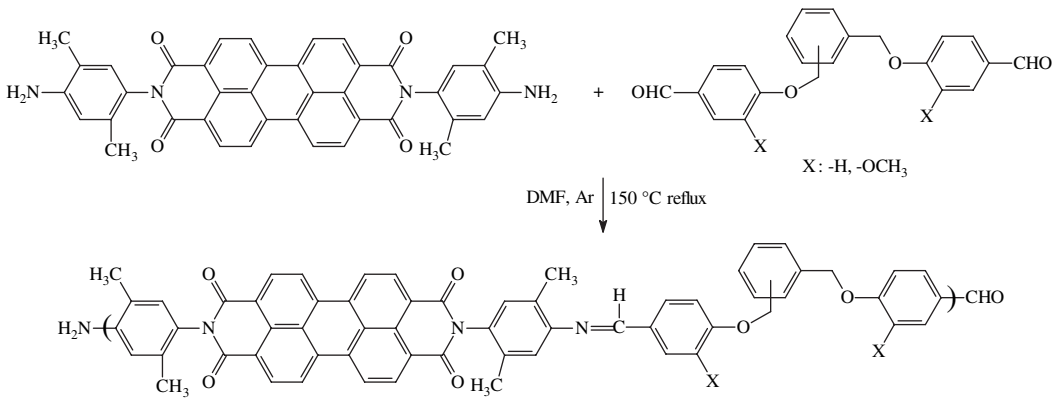

Scheme 3.

fluorescence maxima at 582 nm when they were excited at 535 nm. Optical band gap values (E_g) were calculated from the onset of UV/vis absorption band (Fig. 4), and they were found to be 2.29 eV for whole PAM-PERs (see Table 3).

The electronic properties of the PAM-PERs and the initial compounds were investigated by cyclic voltammetry and Fig. 5 shows the CV voltammograms of them. The cyclic voltammetry measurements were carried out in CH_3CN solution at room temperature and 0.1 M $TBAPF_6$ was used as supporting electrolyte. CV voltammograms of DAs and PAM-PERs were similar to each other. In the cathodic scan region, DAs show single reduction potentials at around −1.89 eV, because of aldehyde groups. Therefore, PAM-PERs and DAPDI show two reversible reduction peaks between −0.46 and −0.72 eV, which reflect the first and second one-electron stepwise reduction process of perylene bisimide (Scheme 4a). Furthermore, PAM-PERs show two irreversible reduction peaks. The first one at around −1.90 eV attributed to the reduction of end group aldehyde carbonyls (−HC═O), and the second one at around −1.80 eV belongs to reduction of repeating imine groups (−HC═N−) in the polymer chain. The reaction mechanism can be proposed as shown in Scheme 4b.

DAs show only one oxidation peak. This peak was observed at around +1.7 eV for DA-1 and DA-2; at around +2.05 eV for DA-3 and DA-4 according to *ortho*- and *para*-position of the phenyl ring in the middle of dialdehydes. On the other hand, DAPDI showed two irreversible oxidation peaks. At the first stage, the amine group was oxidized at 1.46 V and then this charge delocalized over the phenyl ring (Scheme 5b). The second one at +1.77 eV is from perylene core. Finally, PAM-PERs showed only one oxidation peak at around +1.80 eV, which is from perylene core. In the CV voltammograms of DAPDI, the peak at +1.46 eV was observed at lower potential value because of the amine group's electron-donating ability

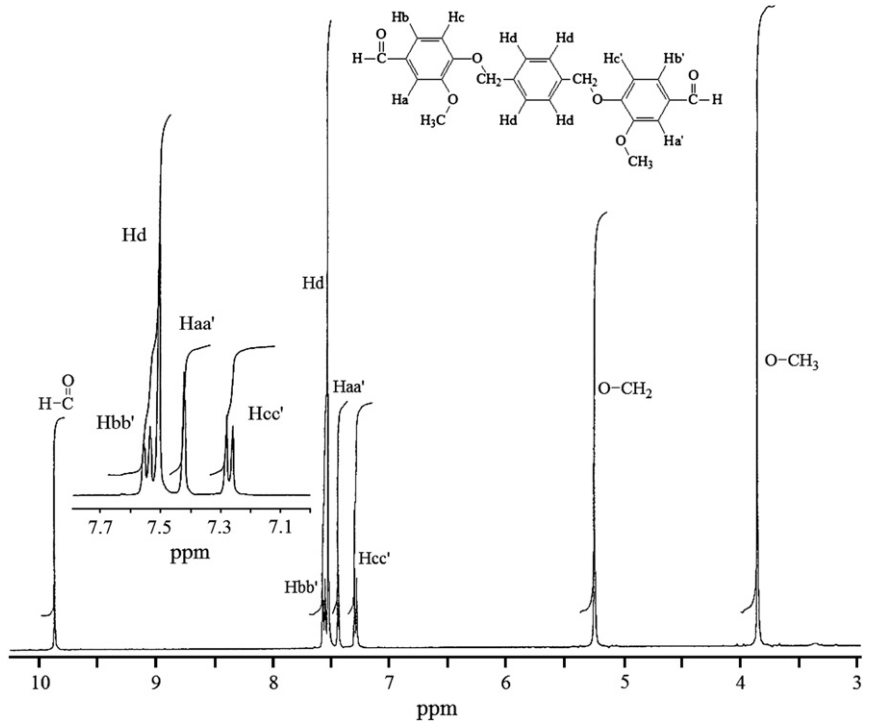

Fig. 1. ^{1}H NMR spectra of DA-1.

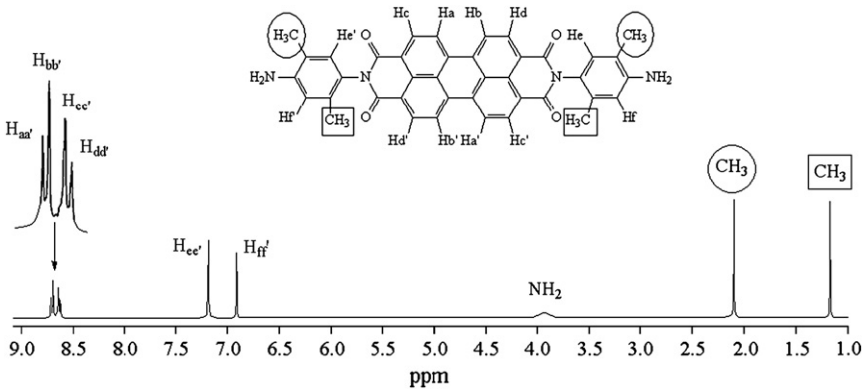

Fig. 2. ^{1}H NMR spectra of DAPDI.

to the phenyl rings. During the polymerization, amine groups ($-NH_2$) on the perylene units converted to imine ($-HC{=}N-$) groups. Because of the withdrawing affect of imine, the peak at +1.46 eV shifted to over +2.2 eV (Scheme 5a–c).

Conductivity measurements of the PAM-PERs were carried out with an electrometer using a four-point probe technique. First of all, conductivity of all the polyazomethines was found to be between 10^{-10} and 10^{-9} S/cm and then an increase was observed after iodine doping. Fig. 6 shows the electrical conductivity results of PAM-PERs under iodine doping in varying periods at 25 °C. Although these molecules are similar to each other, PAM-PER-3 and PAM-PER-4 show higher conductivity than the others. These differences are assumed to be caused by the methoxy groups on the bridging phenyl group. The presence of steric hindrance between methoxy on phenylene group and the carbonyl oxygen of imide forces the 2,5-dimethylphenyl ring to rotate about the N–C bond. As a result of this twisting, there is less available orbital interaction through the nonbonding electron pair orbital of the nitrogen atom. Thus the whole conjugation over the polymer backbone is not fully continuous at all. This uncontinuous conjugation reduces the electrical conductivity. Also, these methoxy groups increase the distance of polymer chains. Since nitrogen is an electronegative element and is capable of coordinating with the iodine molecule, Diaz et al. suggested a conductivity mechanism of imine ($-CH{=}N-$) polymers when doped with iodine [38]. The conductivity mechanism over the polymer backbone can be proposed as shown below (Scheme 6). Both T_g and undoped conductivity values of PAM-PER-1 and PAM-PER-2 were higher than other polymers (see Figs. 6 and 8). But after doped with I_2, conductivities of PAM-PER-1 and PAM-PER-2 were lower than other polymers.

3.3. Thermal analyses

Weight loss data from TGA, DTA and DTG curves of DAPDI and for PAM-PERs are shown in Fig. 7a–c, respectively. These results suggested that 20 and 50% weight loss

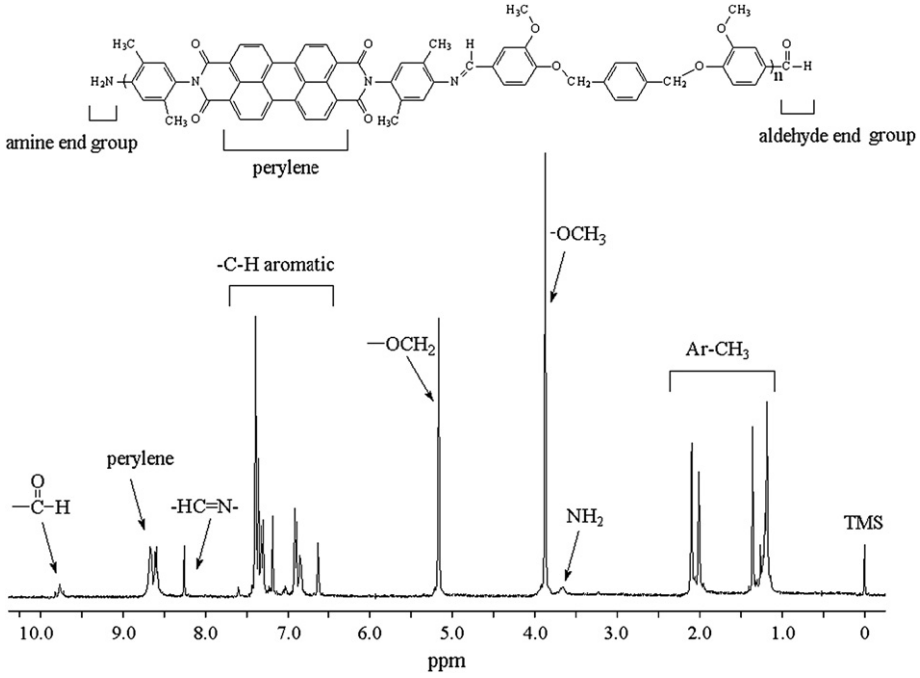

Fig. 3. ^{1}H NMR of spectra PAM-PER-1.

Table 2
The number-average molecular weight (M_n), weight-average molecular weight (M_w), polydispersity index (PDI) and % values of products (PAM-PERs)

Compounds	Total			Fraction I				Fraction II				Fraction III			
	M_n	M_w	PDI	M_n	M_w	PDI	%	M_n	M_w	PDI	%	M_n	M_w	PDI	%
PAM-PER-1	1700	2100	1.235	1680	1880	1.119	67	6700	8900	1.328	32	16,500	17,400	1.055	1
PAM-PER-2	1600	2200	1.375	1250	1800	1.440	62	6450	8700	1.349	38	–	–	–	–
PAM-PER-3	2900	3600	1.241	1660	1840	1.108	83	8900	10,100	1.135	14	198,000	243,000	1.227	3
PAM-PER-4	1300	1500	1.154	1680	1980	1.179	89	13,000	15,300	1.177	9	64,900	66,500	1.025	2

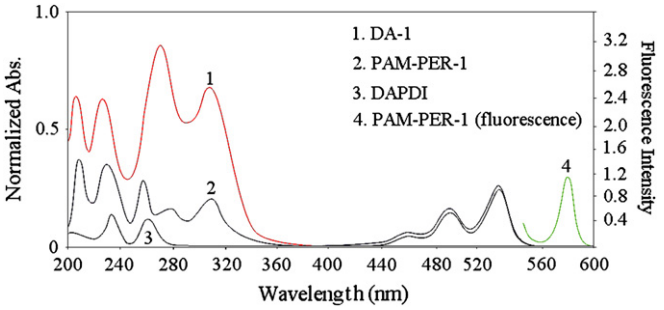

Fig. 4. UV/vis absorption spectra of DA-1, DAPDI and PAM-PER-1 and fluorescence spectra of PAM-PER-1 in chloroform solution.

had occurred in the temperature range of 387–616 °C, 380–566 °C, 400–644 °C and 292–592 °C, for PAM-PER-1, PAM-PER-2, PAM-PER-3 and PAM-PER-4, respectively. PAM-PERs have the onset temperature range from 116 to 231 °C. The TG curves show the major weight loss between 292 and 644 °C, and the residual weight remaining of PAM-PERs at 1000 °C was between 56.21 and 67.28%. This variation in weight loss was due to the differences in the structure of symmetrical and unsymmetrical groups (*para*- or *ortho*-position of benzene ring in the middle of DAs) of PAM-PERs. TGA data indicated that the PAM-PER-1 and

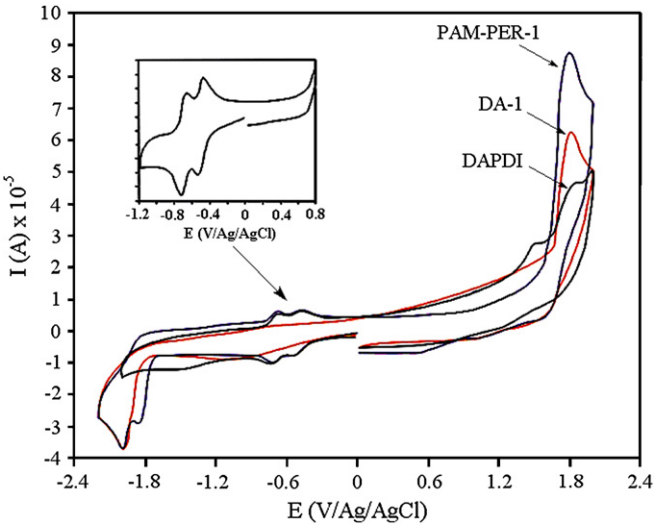

Fig. 5. Cyclic voltammograms of DA-1, DAPDI and PAM-PER-1 in $TBAPF_6$–acetonitrile, scan rate 100 mV s^{-1}.

PAM-PER-3 exhibited higher thermal stability when compared with the others (PAM-PER-2 and PAM-PER-4). According to DTA data of PAM-PERs only PAM-PER-1 showed one exothermic peak. PAM-PER-2, PAM-PER-3 and PAM-PER-4

Table 3
HOMO–LUMO energy levels, electrochemical (E'_g) and optical band gap (E_g) values of initial compounds (DA-1, DA-2, DA-3, DA-4, DAPDI) and products (PAM-PER-1, PAM-PER-2, PAM-PER-3, PAM-PER-4)

Compounds	Reduced groups and peak potentials (V)		Oxidized groups and peak potentials (V)			HOMO (eV)	LUMO (eV)	E'_g (eV)	E_g (eV)
	Aldehyde (–CHO)	–HC=N– (imine)	Perylene (C=O)	Perylene (ring)	Phenyl (ring)				
DA-1	−1.87	–	–	–	+1.72	+5.99	−2.59	3.40	3.63
DA-2	−1.86	–	–	–	+1.74	+5.98	−2.59	3.39	3.63
DA-3	−1.93	–	–	–	+2.08	+6.28	−2.55	3.73	4.01
DA-4	−1.89	–	–	–	+2.09	+6.27	−2.55	3.72	4.01
DAPDI	–	–	−0.46 and −0.52 −0.72 and −0.66 Reversible	+1.77	+1.46	+5.72	−3.98	1.74	2.29
PAM-PER-1	−1.87	−1.82	−0.46 and −0.52 −0.72 and −0.66 Reversible	+1.76	>+2.2	+5.97	−3.98	1.99	2.29
PAM-PER-2	−1.86	−1.80	−0.46 and −0.52 −0.72 and −0.66 Reversible	+1.80	>+2.2	+6.03	−3.98	2.05	2.29
PAM-PER-3	−1.93	−1.81	−0.46 and −0.52 −0.72 and −0.66 Reversible	+1.79	>+2.2	+5.99	−3.98	2.01	2.29
PAM-PER-4	−1.89	−1.79	−0.46 and −0.52 −0.72 and −0.66 Reversible	+1.81	>+2.2	+6.01	−3.98	2.04	2.29

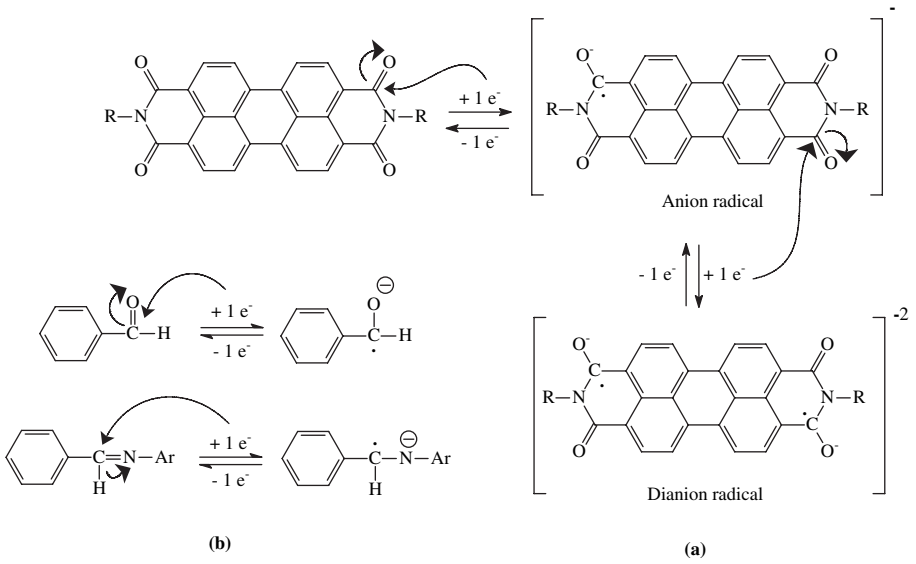

Scheme 4.

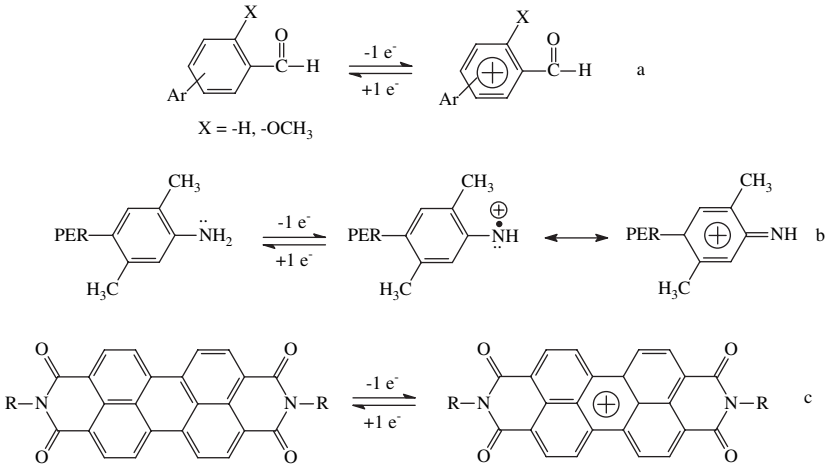

Scheme 5.

displayed neither exothermic nor endothermic peaks. It can be clearly seen that the phenyl ring position has bigger contribution to the thermal decomposition than the existence of the methoxy group in the main chain of PAM-PERs. Based on their similar structures, one may assume that, due to the high temperature, the azomethine (−HC═N−) linkage is the first breaking unit, in all cases.

PAM-PER-1, PAM-PER-2, PAM-PER-3 and PAM-PER-4 formed carbine residues at high amount 43.79, 32.72, 43.35 and 42.19% at 1000 °C, respectively. Because of long band systems, polymers demonstrated higher resistant against high temperature. The initial degradation temperature and the temperature of 20 and 50% weight losses of DAPDI is found to be 161, 311 and 572 °C, respectively. According to DTG curve, thermal degradation of DAPDI occurred in four steps. The weight loss of the first step is found as 11.17% between 100 and 220 °C and of the second step was found as 8.22% between

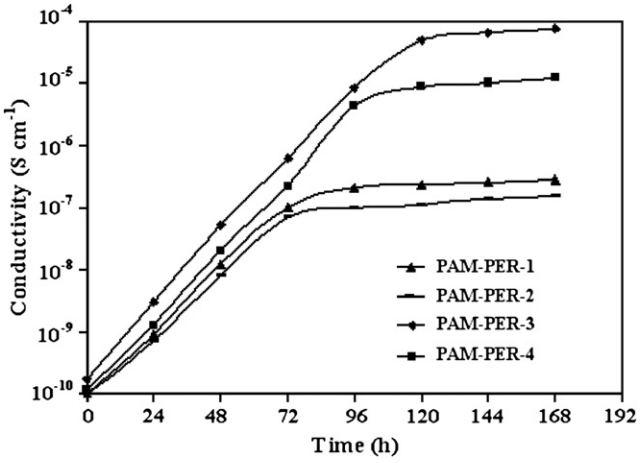

Fig. 6. Change in the electrical conductivities of PAM-PERs during the process of iodine doping at 25 °C.

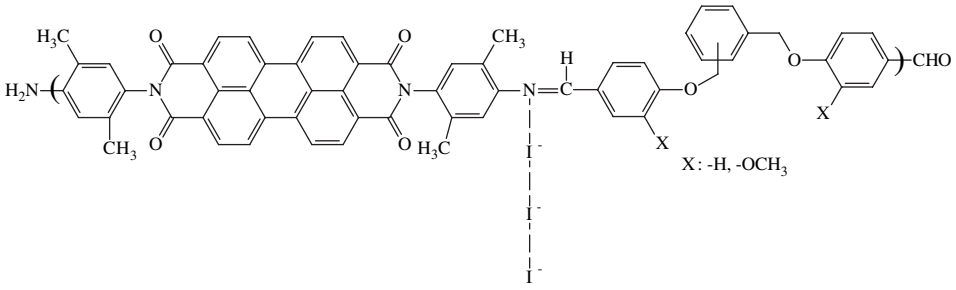

Scheme 6.

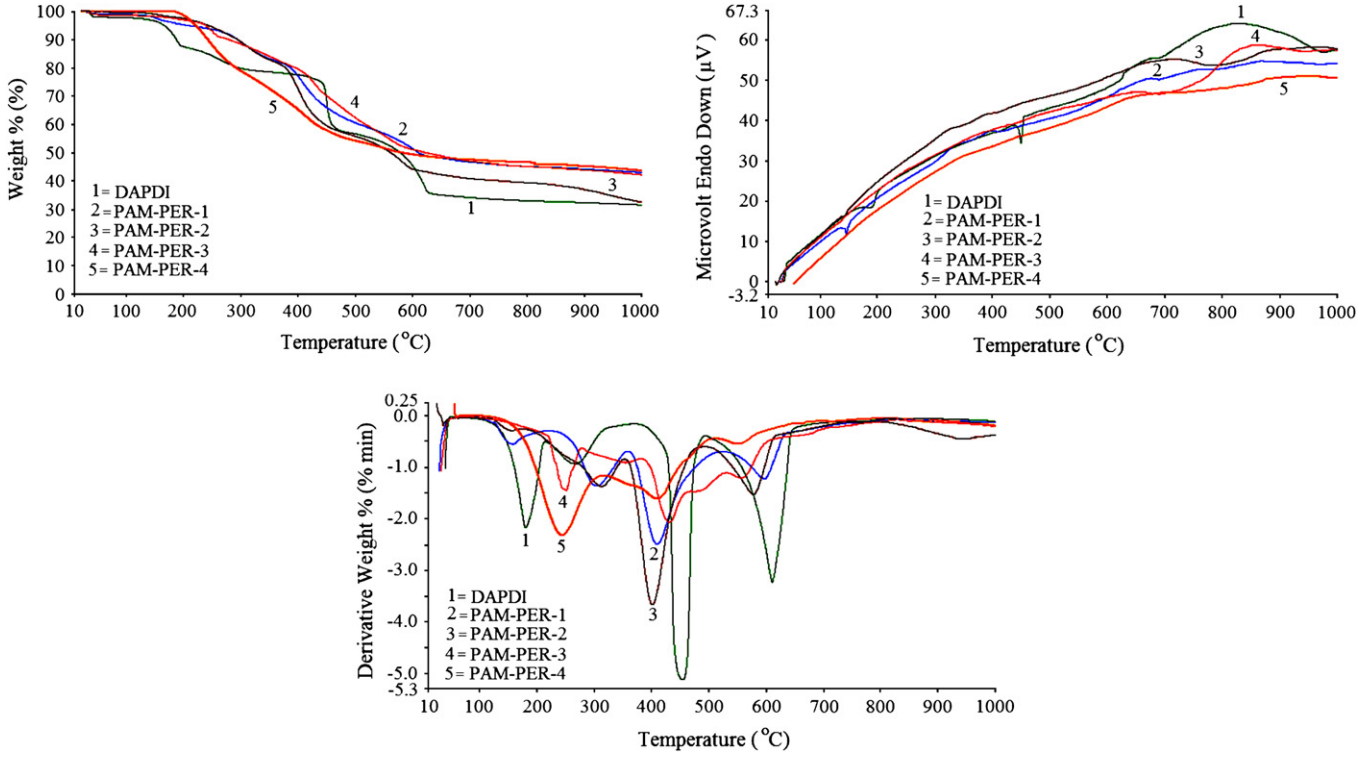

Fig. 7. (a) TGA, (b) DTA and (c) DTG curves of DAPDI and PAM-PERs.

220 and 365 °C. According to DTA analysis, endothermic peak is observed in 188 °C for DAPDI. The initial degradation temperature and the temperature of 20 and 50% weight losses of PAM-PER-1 were found to be 130, 387 and 616 °C, respectively. According to DTG curve, thermal degradation of PAM-PER-1 occurred in four steps and shows the weight loss of the first step was 4.45% between 80 and 220 °C, of the second step was 12.05% between 220 and 360 °C, of the third step was 23.87% between 360 and 525 °C and of the last step was 15.71% between 525 and 1000 °C. Endothermic peak was observed at

Table 4
Thermal decomposition values of DAPDI and PAM-PERs

Compounds	TGA					DTA	DSC
	T_{on} [a]	T_{max} [b]	20% [c]	50% [d]	% carbine residue at 1000 °C	Exo	T_g
DAPDI	161	180, 262, 450, 608	311	572	33.46	188	–
PAM-PER-1	130	155, 302, 408, 595	387	616	43.79	145	145
PAM-PER-2	231	309, 399, 577	380	566	32.72	–	143
PAM-PER-3	210	250, 430, 557	400	644	43.35	–	130
PAM-PER-4	116	242, 409, 551	292	592	42.19	–	128

[a] The onset temperature.
[b] Temperature of the maxima of the peak.
[c] Temperature corresponding to 20 wt% loss.
[d] Temperature corresponding to 50 wt% loss.

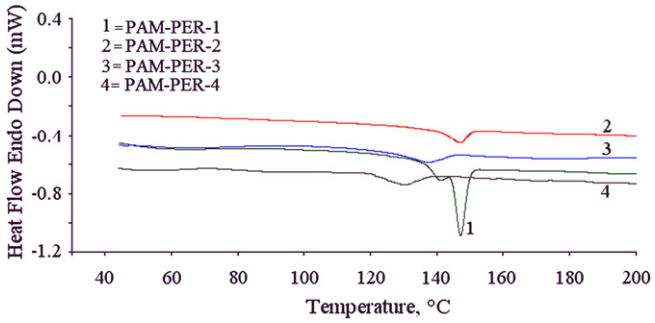

Fig. 8. DSC curves of PAM-PERs.

145 °C for PAM-PER-1. According to DTG curve, thermal degradation of PAM-PER-2 occurred in three steps. The weight loss of the first step was found as 17.11% between 100 and 355 °C, of the second step was found as 26.46% between 355 and 495 °C and last step was found as 23.58% between 495 and 1000 °C. According to DTG curve, thermal degradation of PAM-PER-3 occurred in three steps. The weight loss of the first step was found as 17.75% between 100 and 385 °C, of the second step was found as 22.36% between 385 and 530 °C and of the last step was found as 16.44% between 530 and 1000 °C. According to DTG curve, thermal degradation of PAM-PER-4 occurred in three steps, too. The weight loss of the first step was found as 24.74% between 130 and 320 °C, of the second step was found as 22.64% between 320 and 505 °C and of the last step was found as 10.30% between 505 and 1000 °C (see Table 4). DSC curves of PAM-PERs are given in Fig. 8. According to DSC measurements, glass transition temperature (T_g) values of PAM-PER-1, PAM-PER-2, PAM-PER-3 and PAM-PER-4 were found to be 145, 143, 130 and 128 °C, respectively.

4. Conclusion

Novel polyazomethines containing perylene units in the main chain were synthesized by the condensation reaction of different dialdehydes with *N*,*N*-(2,5-dimethyl-4-aminophenyl)-perylene-3,4:9,10-dicarboximide. Molecular structures of the synthesized compounds were identified by FT-IR, ^{1}H NMR, ^{13}C NMR spectra and elemental analysis and their results showed that all reactions were completed successfully. SEC analyses of all PAM-PERs present low molecular weight and narrow molecular weight distribution. These molecules which have similar electrochemical and optical properties showed different electrical and thermal properties. Thus, after iodine doping, the conductivity of PAM-PER-3 and PAM-PER-4 was higher than of PAM-PER-1 and PAM-PER-2. The results of the TGA–DTA analyses have shown PAM-PERs to have enough resistance against thermal decomposition. The carbine residue of these polymers was observed between 55 and 65% at 1000 °C. According to TG analyses, weight losses of the polymer compounds changed at 1000 °C as follows: PAM-PER-1 > PAM-PER-3 > PAM-PER-4 > PAM-PER-2. Although HOMO–LUMO energy levels and electrochemical band gaps (E_g') of PAM-PERs were found in the range of 1.99–2.04 eV, the optical band gaps (E_g) were measured to be 2.29 eV for all. These results may point that the all molecules can be experimented in photovoltaic devices.

References

[1] Adams R, Bullock RE, Wilson WC. J Am Chem Soc 1923;45:521–7.
[2] Grigoras M, Catanescu CO. J Macromol Sci Part C Polym Rev 2004;C44(2):1–37.
[3] Yang CJ, Jenekhe SA. Chem Mater 1991;3:878–87.
[4] Yang CJ, Jenekhe SA, Vanherzeele H, Meth JS. Chem Mater 1991;3:985–7.
[5] Yang CJ, Jenekhe SA. Chem Mater 1994;3:196–203.
[6] Yang CJ, Jenekhe SA. Macromolecules 1995;28:1180–96.
[7] Marvel CS, Hill WS. J Am Chem Soc 1950;72:4819–20.
[8] Morgan PW, Kwolek SL, Pletcher TC. Macromolecules 1987;20:729–39.
[9] Wojtkonski PW. Macromolecules 1987;20:740–8.
[10] Marvel CS, Tarköy N. J Am Chem Soc 1958;80:832–5.
[11] Marvel CS, Bonsignore PV. J Am Chem Soc 1959;81:2668–9.
[12] Rudzinski WE, Guthrie SR, Cassidy PE. J Polym Sci Part A Polym Chem 1988;26:1677–80.
[13] Barbera J, Oriol L, Serrano JL. Liq Cryst 1992;12:37–47.
[14] Lee KS, Won JC, Jung JC. Macromol Chem 1989;190(7):1547–52.
[15] Park SB, Kim H, Zin WC, Jung JC. Macromolecules 1993;26:1627–32.
[16] Wang C, Shieh S, LeGoff E, Kanatzidis MG. Macromolecules 1996;29:3147–56.
[17] Saegusa Y, Sekiba K, Nakamura S. J Polym Sci Part A Polym Chem 1990;28:3647–59.
[18] Saegusa Y, Takashima T, Nakamura S. J Polym Sci Part A Polym Chem 1992;30:1375–81.
[19] Saegusa Y, Koshikawa T, Nakamura S. J Polym Sci Part A Polym Chem 1992;30(7):1369–73.
[20] Misra M, Das D, Padhi KB, Panigrahi AK, Mohanty AK. J Macromol Sci Pure Appl Chem 1998;A35(5):867–73.
[21] Park KH, Tani T, Kakimoto M, Imai Y. Macromol Chem Phys 1998;199:1029–33.
[22] Hamcium C, Hamcium E, Ronova IA, Bruma M. High Perform Polym 1997;9:177–88.
[23] Bruma M, Schulz B, Töpnick T, Dietel R, Stiller B, Mercer F, et al. High Perform Polym 1998;10:207–15.
[24] Higuchi M, Shiki S, Ariga K, Yamamoto K. J Am Chem Soc 2001;123:4414–20.
[25] Yamamoto K, Higuchi M, Shiki S, Tsuruta M, Chiba H. Nature 2002;415:509–11.
[26] Chernick ET, Mi Q, Kelley RF, Weiss EA, Jones BA, Marks TJ, et al. J Am Chem Soc 2006;128(13):4356–64.
[27] Hara K, Wang ZS, Sato T, Furube A, Katoh R, Sugihara H, et al. J Phys Chem B 2005;109:15476–82.
[28] Neuteboom EE, Van-Hal PA, Janssen RAJ. Chem Eur J 2004;10:3907–18.
[29] Cravino A, Zerza G, Maggini M, Bucella S, Sarıçiftci NS, Maggini M, et al. Chem Commun 2000:2487–8.
[30] Guldi DM, Maggini M, Martin N, Maurizio P. Carbon 2000;38:1615–23.
[31] Pang YH, Xu H, Li XY, Ding HL, Cheng YX, Shi GY, et al. Electrochem Commun 2006;8(11):1757–63.
[32] Hou J, Yang C, Li Y. Synth Met 2005;153:93–6.
[33] Thomas S, Zhang C, Sun SS. J Polym Sci Part A Polym Chem 2005;43:4280–7.
[34] Wagner P, Aubert PH, Lutsen L, Vanderzande D. Electrochem Commun 2002;4:912–6.
[35] Colladet K, Nicolas M, Goris L, Lutsen L, Vanderzande D. Thin Solid Films 2004;7:451–2.
[36] Ahrens AJ, Sinks LE, Rybtchinski B, Liu W, Wasielewski MR. J Am Chem Soc 2004;126:8282–94.
[37] Dodcheva D, Klapper M, Mullen K. Macromol Chem Phys 1994;195:1905–11.
[38] Huang W, Yan D, Lu Q, Huang Y. Eur Poly J 2003;39:1099–104.

[39] Klok HA, Becker S, Schuch F, Pakula T, Mullen K. Macromol Biosci 2003;3:729–41.
[40] Kim DW, Lee CW, Joo SW, Gong MS. J Lumin 2002;99:205–12.
[41] Li CH, Chang TC. J Polym Sci Part A Polym Chem 1990;28:3625–38.
[42] Diaz FR, Moreno J, Tagle LH, East GA, Radic D. Synth Met 1999;100(2):187–94.